High Temperature Magnet Material with Temperature Capability Greater Than 500°C – phase I

Project WBS Number: 694478.02.93.02.13.51.22

Investigator(s): Dr. Jon Goldsby, NASA GRC/RXC, Dr. Sai Raj, NASA GRC/RXC, Dr. Cheryl Bowman, NASAGRC/RXA, Prof. Sivaraman Guruswamy, University of Utah

Purpose

Recent studies have shown that a significant reduction in fuel burn for future aircraft can be achieved by developing hybrid electric airplanes, where an electric motor drives the propeller fan. The fan will be electrically powered by generating electricity using either a gas turbine engine or an energy storage device, such as a battery. For hybrid electric application, the power density for the electric motors has to be increased by a factor of 3-4 compared to the state-of-the-art (SOA). One factor that limits the power density of the permanent magnet electric motors is the temperature capability of permanent magnets. As the motor temperature increases during operation, the SOA magnets lose their magnetic properties. The best high temperature magnetic material available today is $Sm_2(Co,Fe)_{17}$, which has a temperature limit of 400°C for long-duration operation. We propose to develop a high temperature permanent magnetic material with a high Curie temperature and with a capability for using it as a permanent magnet above 500°C for long-duration.

Background

Permanent magnets are unique in their ability to convert energy, whether mechanical to mechanical energy or electric to mechanical energy. They in themselves have no moving parts, no coolant, nor lubrication and hence, inherently a higher reliability. Currently, magnets are developed with trial, error and empirical methods. These commercial magnets are developed with design criteria specific to their application, as an example for automotive or audio service. However, for aviation, the requirements are more stringent and require the magnet to perform in extreme environments. The unique approach to this research is the use of computational methods to find potential high-performing systems, and to filter out alloy compounds, which show little promise for meeting the requirements. In addition, the computational methods also give very good predictions of the materials' properties such as the magnetic moments, its saturation, physical density and stiffness which are relevant to further fabrication.

The proposed effort will enable high power density, non-cryogenic electric motors for hybrid electric aircraft, which will help NASA achieve aggressive (greater than 70 %) fuel burn reduction goals for N+3 (for beyond Yr 2030 time frame) aircraft. The proposed concept will also enable lightweight electromechanical actuation devices for more electric aircraft in the future, with the benefit fuel burn and carbon dioxide emission reduction.

Approach

The approach consists of physics-based computational simulations using the Cambridge Serial Total Energy Package (CASTEP) to identify candidate materials such based on lattice parameters and its electronic configuration as possible high temperature magnet. This is the first time that this material has been identified as a potential magnetic material. Promising materials are fabricated by electric arc-melting of the metal alloy components followed by powder metallurgy processing and testing the high temperature magnetic capability. The appropriate compositions will be arc melted to form the basic ingot. This will be followed by powder metallurgy processing involving crushing, milling, powder compaction and sintering. The samples will then be thermally treated, and microstructure will be examined with the goal of increased magnetic and mechanical durability in extreme environments.

Magnetization measurements on as–cast and powder metallurgy processed samples will be performed using a vibrating sample magnetometer at room and high temperatures to evaluate temperature coefficient coercivity and magnetization. Coercivity is a measure of the magnetic field necessary to demagnetize a permanent magnet. A high coercivity is desirable for long duration and strength. Furthermore, coercivity decreases with an increase in temperature. Therefore, decreasing the coercivity sensitivity to temperature can result in an increase in a permanent magnet's use temperature. A magnet's grain boundaries inhibits the motion of domain walls, hence the coercivity depends on the microstructure which can be controlled using metallurgical techniques. We will also continue to use computational methods to efficiently identify other potential magnetic metal alloys.

Accomplishments

We have made physics-based predictions for the properties of several metallic alloy compounds. We have commenced with the first steps of fabricating some of these materials. Some of the magnets are based on various lanthanide metals -cobalt systems, and others are an attempt to increase temperature capability of the cobalt type magnets. We have successfully installed a large multiprocessor computer to run the materials' computations in a parallel fashion. In addition, we've established a processing protocol to create solid permanent magnetic materials, based upon the results of our physics-based combinatory compositions.

Status of Research

The original proposal calls for the use of the computing facilities, specifically the Pleiades cluster NASA's Advanced Supercomputer at the Ames research center. However, incompatibilities between the firewalls rendered the client-server relationship impractical. We are forced to use a different completing platform consisting of a Hewlett-Packard Z820 desktop workstation is sufficient to carry out the computations of this investigation. The workstation consists of 32 core processors of 64-bit operating system and 32 GB of memory. We're also using the updated version of Accelry's materials studio version 6 as our client interface.

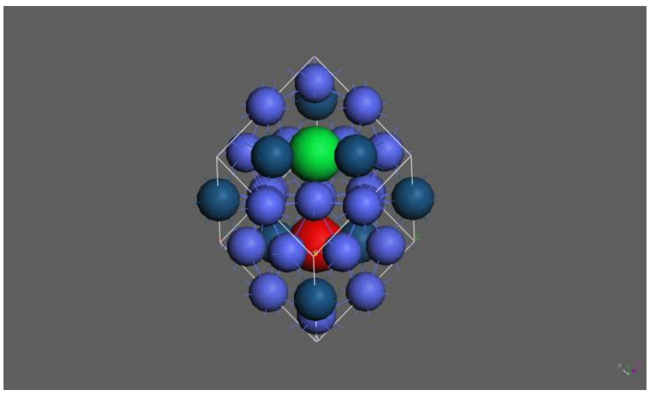

Figure1. Metallic alloy samarium (red), praseodymium (green), cobalt (light blue), iridium (dark blue) system where atoms are rendered as spheres with radii related to van der Waals' radii of the respective atoms.

The original proposal called for the fabrication of the compound Sm_2Ir_{17}, while this compound is hypothetically possible with predicted properties, a study of the binary phase diagram of this system shows no such phase at standard temperatures and pressures can exist. Therefore, this compound will not be synthesized. However, other samarium iridium compounds are stable, such as those listed in **Table 1**. Some of these materials will be further investigated.

Several initial alloys have been calculated and are being investigated as illustrated in **Table I**. **Figure 1** denotes the graphical representation of a metallic alloy samarium, praseodymium, cobalt, iridium system. The relative atomic radii are depicted in this figure. The lanthanide series elements compared to the cobalt host, gives an indication of the qualitative measure of the thermal energy needed for homogenization.

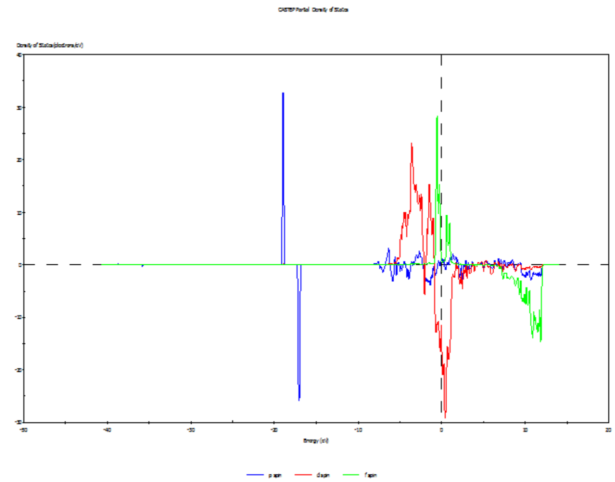

Figure 2. Calculated density of electron states (orbitals: d-red, f-green, p- blue) spin decomposed and symmetry-resolved illustrating the difference between the spin up (positive) and spin down (negative) electron states, which give rise to the ferromagnetism of this alloy.

Figure 2 gives a density of states of the alloys explicitly illustrating the net spin of the electron states. The dotted vertical line denotes the Fermi level of this material. The participating electron orbitals are hybridized with the s, d and f orbitals electrons being the most dominant in contributing to the material's magnetic moment.

Alloys	Bulk Modulus GPa	Density g/cm3	Lattice Parameter Angstrom	Magnetic Moment Bohr Magenton
Sm5Ir3	31	10.30	a=b=11.4 c=6.8	122
Sm2Ir17	354	10.69	a=6.47	36.5
Gd2Co17	239	9.02	a=b=8.29 c=8.13	76
GdPrCo	260	8.38	a=6.41	36
SmPrCoIr	500	11.00	a= 6.42	32

Table 1. Predicted material parameters of various ferromagnetic compounds.

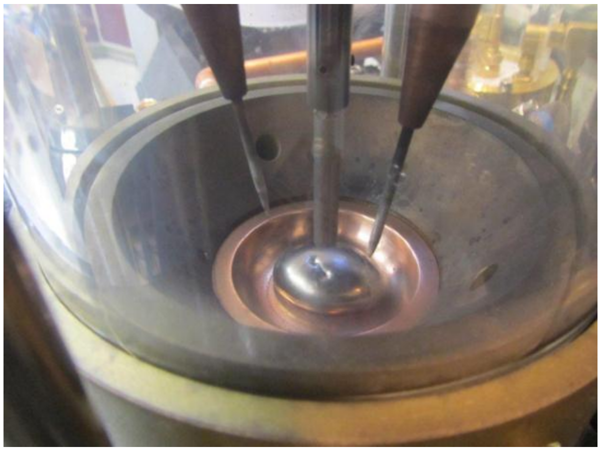

Figure 3. View through the Pyrex observation port with a melted metallic alloy sample on the copper hearth with 2 mm diameter tungsten electrodes suspended from above.

Once a composition is selected a pilot charge, consisting of 10 to 20 g was fabricated. High- purity metals are consolidated in an electric arc furnace (**Figure 3**). The pilot charge is placed on a water-cooled copper hearth. As such, minimal contamination can be anticipated. Tungsten electrodes powered by a heavy-duty cycle welding power source, deliver 60 to 100 amperes of current to melt the sample. To aid in mixing, the samples are flipped several times and re-melted. The entire melting sequence is carried out under flowing argon gas to prevent oxidation. The samples are subsequently homogenized at various temperatures and times from two 100 hours at two-thirds of the melting temperature of the constituent materials. A mechanical pump is used to evacuate a glass tube (sealed at one end and connected to the gas/vacuum line at the other) to less than about 0.1 Torr. The tubing is then backfilled with ultra-high purity argon to +5 psi and evacuated, and the cycle is repeated about 15 times before the sealing is done. The vial length is about 4 inches so that the sample is not heated during sealing. With annealing time, the magnetization observed should increase and saturates at some time duration, typically within 48 hours. The annealed ingot sample was then milled wet in a protective kerosene fluid using a SPEX mill using s stainless steel container with 6 mm stainless steel balls as milling media. Milling durations were between 30 and 75 minutes. The particle size of the powder after milling the bulk alloy material is given in **Figure 4**. In this case, a particle size on the order of 10 μm was obtained.

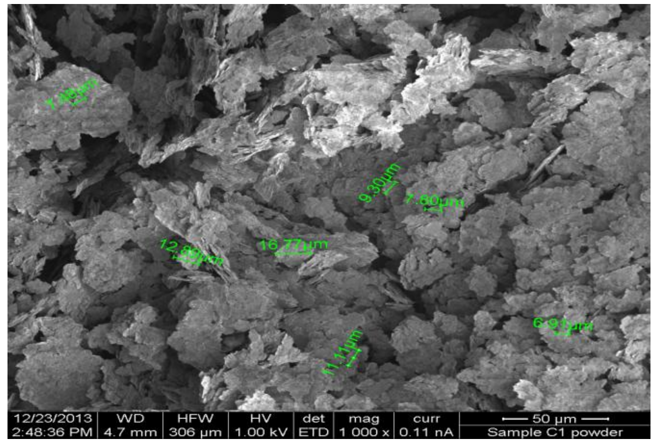

Figure 4. A micrograph of milled praseodymium gadolinium cobalt alloy powder before cold pressing and sintering.

After milling, the kerosene was decanted. The powder was then washed in acetone and methanol, and stored in a sealed container. Pellets (6 mm diameter x 6 mm high) were formed using a polyethylene glycol bind Alloy powders were dissolved initially in acetone as a lubricant/binder (1 1.5 wt. %) Cold pressed with 1500 kg/cm^2 Heated under argon gas to 325^{o}C to remove the binder 12 or 13 mm Id and thick walled quartz tube sealed using oxyacetylene torch **Figure 5**. Green body pellets were then sealed under argon in a quartz vial and sintered 1190^{o}C for several hours. Magnetic measurements were made using a vibrating sample magnetometer.

Figure 5 Sealed quartz tube containing cold a pressed alloy pellet ready for sintering.

Increase of 25 % in magnetic moment over similarly processed SmCo Excellent magnetic properties to 700^{o}C Density functional theory allows prediction of properties for magnetic alloys. Further development is needed to include finite temperature predictions for more complicated alloy systems. Coercivity and temperature insensitivity not as good as SmCo, however better process control is needed for a definitive answer

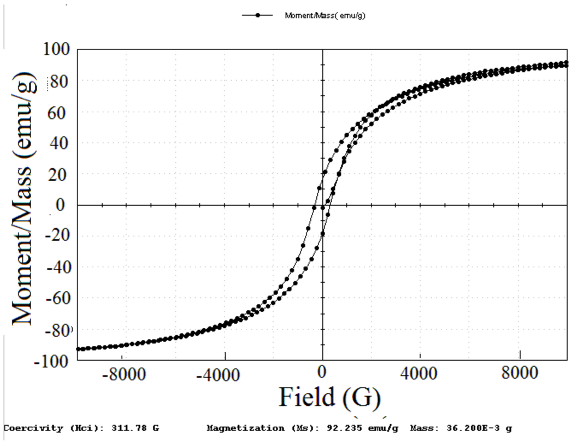

Figure 6. The hysteresis curve for the annealed $GdPrCo_{17}$ coarse powder.

Magnetization measurement of a gadolinium, praseodymium, cobalt ($GdPrCo_{17}$) alloy powders obtained after annealing cast ingot and coarsely milling to a powder with an average size of about 30 µm, was conducted with a Lakeshore 7307 vibrating sample magnetometer. The hysteresis curve obtained from this measurement is shown in **Figure 6** gives the saturation magnetization and coercivity of the new ferromagnetic compound. The preliminary results of the magnetization reveal a saturation value of 93 emu/g (electromagnetic units/gram) at an applied external magnetic field of 9975 Gauss. Further improvements are expected with additional processing.

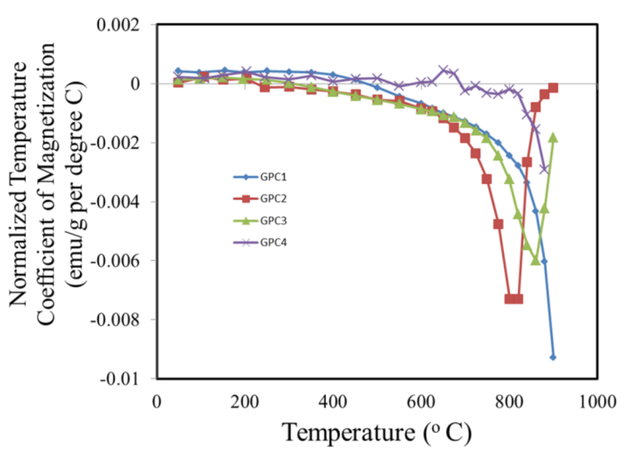

Figure 7. Temperature stability of magnetic properties.

The normalized temperature of the specific magnetization (**Figure 7**) remains near zero for all of the alloys tested with the (Sm,Pr,Gd,Er,Ce)Co material demonstrating the most significant deviations at temperatures above 650°C with a value of -2×10^{-3} emu/g* °C, while the samarium cobalt test standard remains constant up to 800°C. It appears that the alloys with fewer components, exhibits the greater stability, while the multi-component alloys show the least amount of stability. This component-dependent instability may indicate processing related non-uniform alloy mixing. **Table II** gives the calculated compositions for the various charge weights and the actual compositions. The results indicate very little material has been lost due to the electric arc melting process.

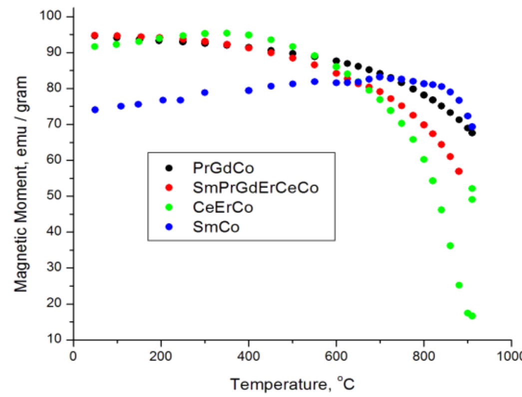

Figure 8. Comparison of temperature dependent magnetic moments.

Figure 8 illustrates the mass specific magnetic moments for the various alloys fabricated. We also produce as a standard a samarium cobalt composition, which was processed identically to the candidate materials. The room-temperature moment of all the alloys exceeds that of the samarium cobalt composition by over 25 percent. However, as the temperature increases beyond 650°C, the magnetic moments tend to converge at 85 emu/g. Temperatures above 650°C and below the Curie temperature, values of all the alloys decreased.

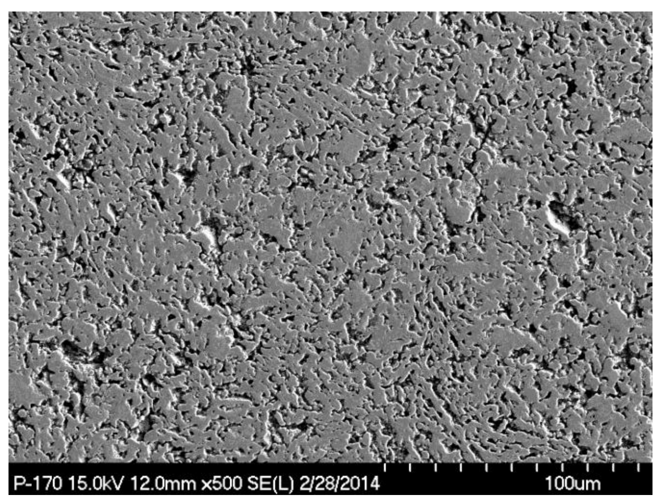

Figure 9. Micrograph of $(PrGd)Co_{17}$

Figures 9 and **10** give post-processed microstructural information for alloy (Pr,Gd)Co17, which we believe to be the most promising composition. **Figure 9** gives an overall view of the material, immediately evident is the relatively high porosity. First-principle calculations for a single crystal, predicts a density of 8.3 g/cm³, however the final processed and tested density is 4.29 g/cm³, thereby yielding a material with 48% porosity.

To determine the compositions within the various phases, energy dispersive spectroscopy (EDS) was used. The spectrum reveals concentrated areas of praseodymium and gadolinium within the cobalt matrix (**Figure 11**). High lanthanide concentrations, such as these, indicates that the electric arc-melting process used in this study, even with maximum applied currents of 400 amperes were not sufficient to melt and homogenize the magnetic alloys to a satisfactory level. In addition, the porosity found in the post-sintered material means full density cannot be achieved with mere sintering. Alternative methods for melting and consolidating the components, such as electric induction heating and pressure assisted sintering (hot pressing) will likely yield a more uniform and even distribution within the material and improved density. These methods will be used in future studies.

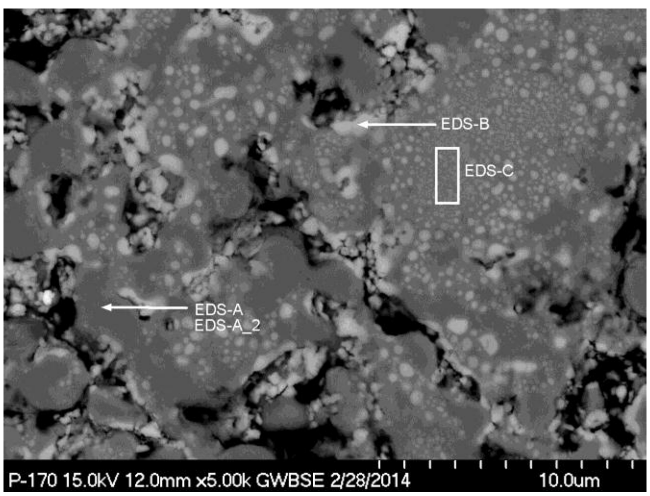

Figure 10. Micrograph of (PrGd)Co_{17} showing lanthanide metal concentrations.

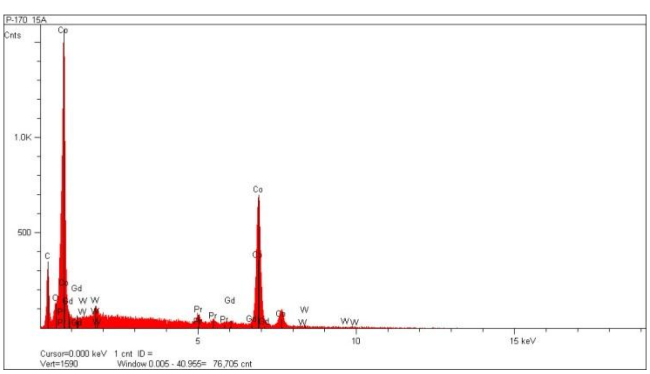

EDS-A

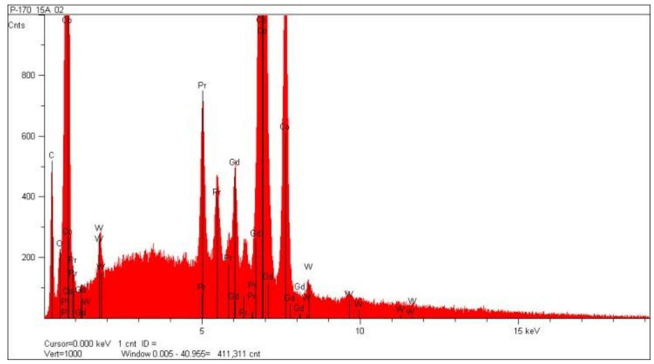

EDS A-2

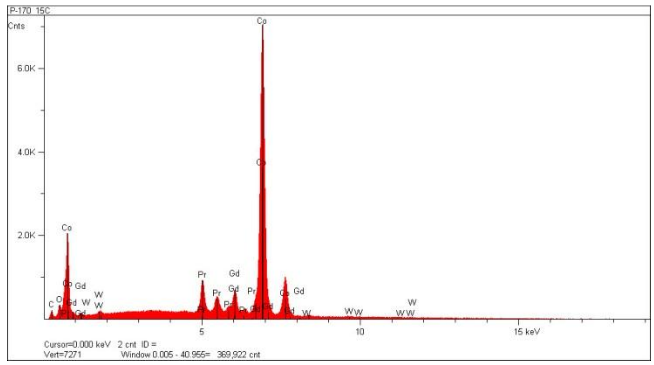

EDS C

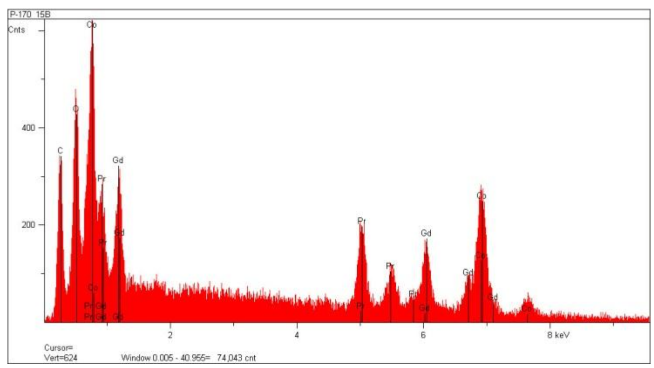

EDS B

Figure 11. Compositions within the various phases using energy dispersive spectroscopy (PrGd)Co_{17}

	Sm	Er	Ce	Al	Mg	Pr	Gd	Co
(Pr,Gd)Co17	*	*	*	*	*	10.8 (11.2)	12.1 (12.7)	77.1 (76.1)
(Sm,Gd,Er,Ce)(Co,Al,Mn)	4.18 (3.7)	5.93 (5.8)	3.94 (4)	0.697 (0.7)	1.545 (1.2)	*	5.06 (5.0)	78.6 (79.5)
(Ce,Er)Co17	*	12.79 (12.3)	10.75 (11.0)	*	*	*	*	76.5 (76.6)

Table II Nominal alloy compositions in wt% and analytical results in parenthesis.

Current TRL: 2

Applicable NASA Programs/Projects

High-temperature magnets are planned into a proposed new effort for hybrid-electric propulsion in the subsonic fixed-wing project in the aerosciences projects.

Publications and Patent Applications
NASA TM and peer-reviewed publication .journal are planned from this research.

Awards & Honors related to Seedling Research
None at this time.